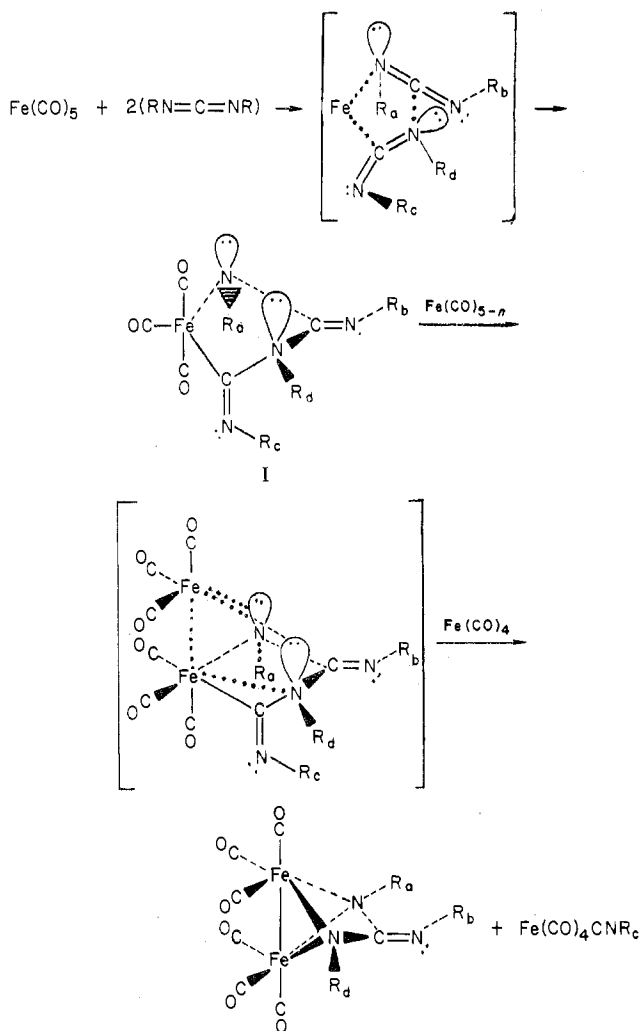


Scheme I



We shall show in future reports how the occurrence of asymmetric metalocycles also accounts for the isomeric distribution where two different cumulenes are coupled together.

References and Notes

- (1) N. J. Bremer, A. B. Cutcliffe, M. F. Farona, and W. G. Kofron, *J. Chem. Soc. A*, 3264 (1971).
- (2) J. D. Cotton and S. D. Zornig, *Inorg. Chim. Acta*, **25**, L133 (1977).
- (3) T. Herskowitz and L. J. Guggenberger, *J. Am. Chem. Soc.*, **98**, 1615 (1976).
- (4) J. E. Bercaw and D. M. Duggan, submitted for publication.
- (5) J. R. Schmidt and D. M. Duggan, submitted for publication.
- (6) G. Fachimetti, C. Biran, C. Floriani, A. Chiese-Villa, and C. Guastini, *J. Am. Chem. Soc.*, **100**, 1921 (1978).
- (7) J. Chatt, M. Kubota, G. J. Leigh, F. C. March, R. Mason, and D. J. Yarrow, *J. Chem. Soc., Chem. Commun.*, 1033 (1974).

Department of Chemistry
University of California
Irvine, California 92717

D. Michael Duggan

Received July 21, 1978

Nature of the Jahn–Teller Effect in the $\text{Cu}(\text{C}_5\text{H}_5\text{NO})_6^{2+}$ Ion

Sir:

On the basis of recent independent studies, Carlin, O'Connor, and Sinn¹ and the present authors² have reported the

single-crystal ESR spectra of the copper-doped hexakis-(pyridine *N*-oxide) complex of zinc and have interpreted the results in terms of static and dynamic Jahn–Teller effects, respectively. Carlin and co-workers also report the results of complete X-ray structure analyses of the perchlorate and tetrafluoroborate salts of both copper and zinc complex ions, and these confirm the earlier conclusions³ that these four compounds are isostructural with the cobalt and nickel complexes whose structures had previously been determined.^{4,5} Since the metal ion site symmetry in all of these structures at ambient temperature is S_6 (space group $R\bar{3}$), the copper(II) salts afford additional examples of those hexacoordinated compounds of this ion whose structures apparently have a higher symmetry than that allowed by the Jahn–Teller theorem.

The single-crystal ESR spectra for such trigonal and cubic copper complexes are generally temperature dependent, indicating that the Jahn–Teller effect is dynamic on the ESR time scale at ambient temperature. As the temperature is reduced, however, the isotropic or near-isotropic signal corresponding to the "averaged" structure is usually replaced by spectra characteristic of three magnetically inequivalent sites related by the crystal threefold axis. This dynamic to static transition is generally interpreted in terms of the model proposed by Abragam and Pryce,⁶ each site in the low-temperature spectra (i.e., below the transition point) representing a minimum in the Jahn–Teller potential wells and having magnetic parameters corresponding to the tetragonally elongated geometry typical for copper. The transition temperature is ligand dependent, ranging from 12–50 K for $\text{Cu}(\text{H}_2\text{O})_6^{2+}$ to ca. 200 K for the tris(octamethylpyrophosphoramid)copper(II) ion⁸ and the $\text{Cu}(\text{NCH})_6^{2+}$ ion. The presence or absence of hyperfine structure in the higher temperature spectra is also ligand dependent.

Such features as described are evident in the spectra obtained for the $\text{Cu}(\text{C}_5\text{H}_5\text{NO})_6^{2+}$ complex doped into the corresponding zinc lattice, and our initial studies, carried out on crystals grown from dimethylformamide–ethanol solutions and using spectra recorded over a temperature range at both X- and Q-band frequencies, were interpreted in the framework of this model.² The transition temperature, as derived from the spectra measured at X-band frequency, was found to be in the region of 50 K. However, the interpretation of these ESR spectra was made more complicated than for those reported for previous examples by the observation of additional sites, suggesting the presence of different types of copper ion geometry in the host crystal. The spectra indicated two sets of three magnetically inequivalent sites, related by the crystal threefold axis, together with the near-isotropic signal, characteristic of the dynamic Jahn–Teller effect, which in the crystals examined¹⁰ accounted for the largest fraction of the total intensity of the spectra.

While the near-isotropic signal diminished in intensity on cooling, being replaced at ~ 50 K by signals for the three sites exhibiting a static Jahn–Teller effect, the additional sites (which, in contrast to the isotropic signal, showed the characteristic four-line hyperfine splitting pattern for copper) were affected very little by the temperature change but showed marked angular variations. The rotational behavior and line-width variation of the near-isotropic signal, on the other hand, parallel very closely that observed for the pure $\text{Cu}(\text{C}_5\text{H}_5\text{NO})_6^{2+}$ complex, which at room temperature gives only an exchange-narrowed line.

In contrast with our interpretation of the main features of these spectra in terms of the dynamic \leftrightarrow static Jahn–Teller effect, however, Carlin, O'Connor, and Sinn¹ discuss their X-band room-temperature ESR results solely in terms of three statically distorted sites related by the crystal threefold axis.

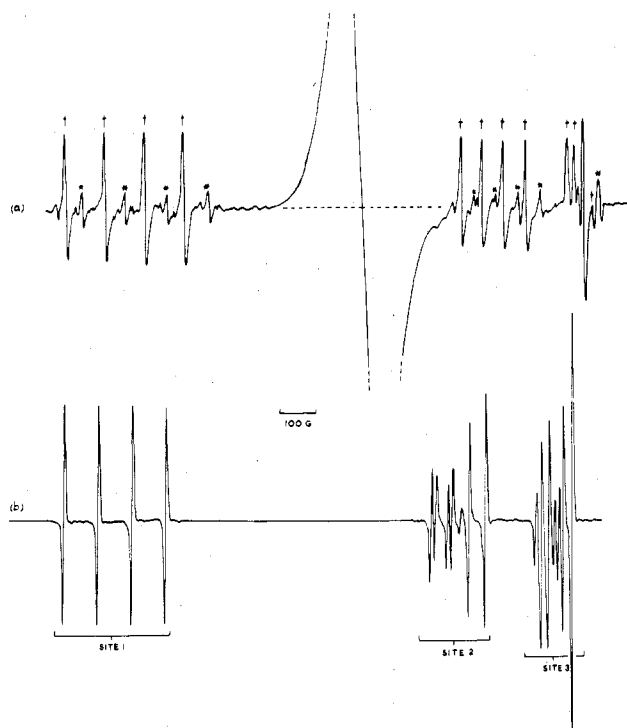


Figure 1. Q-Band ESR spectra at (a) room temperature (295 K) and (b) 20 K of a 2% ^{63}Cu -doped single crystal of $\text{Zn}(\text{C}_5\text{H}_5\text{NO})_6(\text{BF}_4)_2$ grown from acetonitrile solution (arbitrary crystal orientation). The additional sites arising from the solvated species are indicated in spectrum (a); the sets of lines denoted * are assumed to arise from the three magnetically nonequivalent sites occupied by $\text{Cu}(\text{C}_5\text{H}_5\text{NO})_4(\text{MeCN})_2^{2+}$ complexes while those sets denoted by the asterisk are assigned to the monosolvated complexes. In contrast to the spectra obtained for crystals from DMF solution,² these additional sites are not observable in the low-temperature spectra.

Thus, their conclusion is that the Jahn–Teller effect is static on the ESR time scale, while it is dynamic on the X-ray time scale. As they indicate, this would be the first observation of such a phenomenon.¹¹

It is the purpose of this correspondence, therefore, to point out that the $\text{Cu}(\text{C}_5\text{H}_5\text{NO})_6^{2+}$ ion does not in fact present any new features with regard to the nature of the model for the dynamic–static Jahn–Teller effect and that, when doped in the corresponding zinc host lattice, the ion exhibits a static effect below 47 K and a dynamic effect above that temperature with an exchange frequency which, at room temperature, lies between the time scales of the ESR and infrared techniques.¹² Examination of the magnetic parameters (which indicate marked deviation from axial symmetry) and angular variation of g values reported by Carlin et al. reveals that the near-isotropic line has been assumed to arise from one of the three statically distorted sites and has been used in conjunction with the lines from the additional sites to obtain the reported results.

Our initial interpretation of the stronger of the additional two sets of three room-temperature sites was that they arose from a small proportion of $\text{Cu}(\text{C}_5\text{H}_5\text{NO})_6^{2+}$ ions having D_{4h} geometry and exhibiting a static Jahn–Teller effect in the host lattice, while the second and weaker set was attributed to a solvated species, in which one or more pyridine *N*-oxide ligands had been replaced by (presumably) DMF molecules.² However, further ESR studies, using crystals grown from different solvents, have now resolved what was initially a puzzling question, namely, the apparent presence of a small proportion of the $\text{Cu}(\text{C}_5\text{H}_5\text{NO})_6^{2+}$ ions in the zinc lattice exhibiting a static Jahn–Teller effect with the simultaneous presence of the majority engaged in a dynamic–static Jahn–Teller equilibrium. These additional measurements

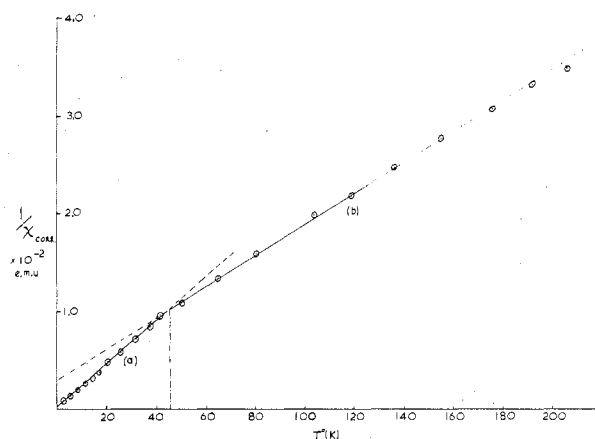


Figure 2. Curie–Weiss plot of the inverse susceptibility of $\text{Cu}(\text{C}_5\text{H}_5\text{NO})_6(\text{ClO}_4)_2$. The Weiss constants for the two branches of the plot are (a) -2.4 K and (b) -18.5 K. For the BF_4 salt, the intersection of the two plots is at 50 K and the Weiss constants are very similar to those for the ClO_4 salt.

strongly suggest that both of these extra sites arise from solvated species, probably $\text{Cu}(\text{C}_5\text{H}_5\text{NO})_5\text{S}^{2+}$ and $\text{Cu}(\text{C}_5\text{H}_5\text{NO})_4\text{S}_2^{2+}$, which are apparently formed during the crystal-growing process. In the room-temperature spectra, therefore, only the near-isotropic signal is attributable to the hexakis(pyridine *N*-oxide) complex.

Crystals grown from acetonitrile solution illustrate these points quite clearly, and sample room- and low-temperature spectra obtained from 2% doped crystals are illustrated in Figure 1. Both sets of additional sites appear in the room-temperature spectra, but they have much lower intensity relative to that of the near-isotropic signal than is found for the crystals grown from dimethylformamide–ethanol solution. Moreover, they appear to be characterized by slightly different g and A values. On the other hand, the position of the near-isotropic signal and its temperature-dependent behavior are the same for crystals grown from either acetonitrile or DMF solution. Measurements at Q-band frequency show that the dynamic to static transition occurs over the temperature range 105–47 K for the crystals with ClO_4^- as anion but much more sharply and within the range 55–47 K for crystals with BF_4^- as anion.

In contrast to the spectra of the copper complexes doped into the zinc lattice, whose spectra exhibit the same three-site behavior below the transition temperature for both BF_4^- and ClO_4^- salts, the low-temperature spectra of the pure tetrafluoroborate and perchlorate salts differ considerably and suggest the presence of a cooperative Jahn–Teller effect which gives different low-temperature structures for the two salts. Although the transition temperature is very similar for both salts and lies in the range 45–55 K, for crystals of the perchlorate salt obtained from DMF solution, we find a near-isotropic signal described by an axial g tensor aligned with the trigonal crystal axis, while for the tetrafluoroborate complex, also obtained from DMF solution, three magnetically nonequivalent sites related by the crystal C_3 axis are produced as for the doped systems. However, the populations of the three sites, as indicated by their relative intensities in the ESR spectra, are dramatically different, with one site predominating over the other two. Preliminary indications suggest that these results¹³ are in accord with a model involving ferro-distortive ordering of the tetragonally elongated octahedra for the BF_4^- salt below the transition temperature and antiferro-distortive ordering for the ClO_4^- salt, and these conclusions are in agreement with the low-temperature magnetic specific heat measurements of de Jongh and co-workers.¹⁴

Additional evidence for the occurrence of a first-order phase

transition in the pure copper complexes and for the close similarity of the transition temperatures in the ClO_4^- and BF_4^- salts is obtained from bulk susceptibility measurements in powder samples. Figure 2 illustrates a Curie-Weiss plot for the perchlorate salt and indicates that the susceptibility cannot be adequately described with a single Weiss constant. The plot for the tetrafluoroborate salt is essentially the same.

A similar well-defined phase transition has been observed in the temperature variation of the single-crystal magnetic anisotropy of $\text{Cu}(\text{en})_3\text{SO}_4$,¹⁵ and the transition temperature correlates very well with that observed for the dynamic to static change in the ESR spectra.

Acknowledgment. J.S.W. is grateful to the University of Nijmegen for hospitality extended to him during a sabbatical leave (1976-1977) and we thank the Scientific Affairs Division of NATO for their support of this project.

Registry No. $\text{Cu}(\text{C}_5\text{H}_5\text{NO})_6(\text{ClO}_4)_2$, 14245-15-9; $\text{Zn}(\text{C}_5\text{H}_5\text{NO})_6(\text{BF}_4)_2$, 23013-69-6; $\text{Cu}(\text{C}_5\text{H}_5\text{NO})_4(\text{MeCN})_2^{2+}$, 68876-54-0.

References and Notes

- (1) R. L. Carlin, C. J. O'Connor, and E. Sinn, *Inorg. Chem.*, **16**, 3314 (1977).
- (2) C. P. Keijzers, E. de Boer, and J. S. Wood, *Chem. Phys. Lett.*, **51**, 489 (1977).
- (3) D. Taylor, Australian National University, private communication; A. D. Van Ingen Schenau, Ph.D. Thesis, University of Leiden, 1976.
- (4) T. J. Bergendahl and J. S. Wood, *Inorg. Chem.*, **14**, 338 (1975).
- (5) A. D. Van Ingen Schenau, G. C. Verschoor, and C. Romers, *Acta Crystallogr., Sect. B*, **30**, 1686 (1974).
- (6) A. Abragam and M. H. L. Pryce, *Proc. Phys. Soc., London, Sect. A*, **63**, 409 (1950).
- (7) B. Bleaney and K. D. Bowers, *Proc. Phys. Soc., London, Sect. A*, **65**, 667 (1952).
- (8) R. C. Koch, M. D. Joesten, and J. H. Venable, Jr., *J. Chem. Phys.*, **59**, 6312 (1973).
- (9) W. L. Driessen, *Inorg. Nucl. Chem. Lett.*, **12**, 873 (1976).
- (10) The intensities of the signals attributed to the additional sites relative to that of the isotropic signal appear to depend both on the amount of copper complex in the zinc host and on the rate of crystal formation.
- (11) While the X-ray results for such octahedral copper complexes are compatible with the occurrence of a dynamic Jahn-Teller effect, they do not exclude a situation in which each complex is trapped in one of three mutually orthogonal (or near orthogonal) tetragonal distortions, i.e., a space-averaged, as opposed to a time-averaged disorder. Although the interaction time in the X-ray experiment is much shorter than the time required to execute a molecular vibration, the integration over the time necessary to accumulate significant intensity results in the diffraction experiment being unable to distinguish between either disorder model. That such models are compatible with the X-ray structural data in the present situation is evident in comparing the published thermal parameters for the copper and zinc complexes given in ref 1. For both ClO_4^- and BF_4^- salts, the largest root-mean-square displacements lie almost directly along the Cu-O bonds, while in the zinc complexes, the largest displacements are normal to the Zn-O bonds.
- (12) A. T. Hutton and D. A. Thornton, *J. Mol. Struct.*, **39**, 33 (1977). The infrared spectra of the copper complexes in the region of the M-O and N-O stretching vibrations indicate a tetragonally distorted (D_{4h}) geometry.
- (13) E. de Boer, C. P. Keijzers, and J. S. Wood, to be submitted for publication. ESR studies of single crystals of the pure complexes obtained from different solvents indicate that the solvation plays an important role here as for the doped systems.
- (14) H. A. Algra, L. J. de Jongh, and R. L. Carlin, *Physica B: + C (Amsterdam)*, **93 B + C**, 24 (1978). These studies show the magnetic structure to be an assembly of weakly coupled antiferromagnetic layers for $\text{Cu}(\text{C}_5\text{H}_5\text{NO})(\text{BF}_4)_2$ and chains for $\text{Cu}(\text{C}_5\text{H}_5\text{NO})_6(\text{ClO}_4)_2$.
- (15) S. N. Mitra and P. Sengupta, *Indian J. Phys.*, **47**, 79 (1973).

Department of Chemistry
University of Massachusetts
Amherst, Massachusetts 01003

John S. Wood*

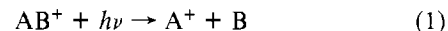
Department of Molecular Spectroscopy
University of Nijmegen
Nijmegen, The Netherlands

E. de Boer
C. P. Keijzers

Gas-Phase Photodissociation of $(\eta^5\text{-C}_5\text{H}_5)\text{NiNO}^+$

Sir:

Ion cyclotron resonance spectroscopy^{1,2} (ICR) has proven to be invaluable in the study of gas-phase ion photochemistry. In particular, by monitoring photodissociation process 1 as a



function of wavelength, the photoexcitation spectrum is obtained. From such studies, a wide range of spectroscopic, thermodynamic, kinetic, and dynamic information about ions can be derived.³⁻⁸ While numerous photochemical studies utilizing ICR have been reported for organic ions, only a few studies have been reported for ions generated from transition-metal complexes. The latter studies have been limited to transition-metal carbonyl anions and have yielded mainly interesting qualitative information.^{7,8}

In this paper we report application of ICR photodissociation techniques to determining the binding energy of NO to $(\eta^5\text{-C}_5\text{H}_5)\text{Ni}^+$, hereafter referred to as CpNi^+ , and to the determination of two low-lying excited states of CpNiNO^+ which indicate the potential of this method for obtaining such quantitative, as well as qualitative, information about this important class of compounds.

The availability of the photoelectron spectrum of CpNiNO^9 and a precise determination of $D(\text{NO-CpNi}^+) = 45.9 \pm 1.0$ kcal/mol obtained recently from photoionization experiments¹⁰ in conjunction with elegant ICR trapped-ion gas-phase equilibrium measurements¹¹ made CpNiNO^+ a logical candidate for initiating our photochemical studies in this exciting area.

The cyclopentadienylnickel nitrosyl parent ion, CpNiNO^+ , was generated from the neutral compound at an electron energy of 20 eV. Trapping times were typically 1.5 s and CpNiNO pressures were $\leq 1 \times 10^{-7}$ torr. Upon irradiation, the parent ion undergoes photoreaction 2. Interference from



other species present¹¹ was not observed. The photodissociation spectrum of CpNiNO^+ , obtained by monitoring the disappearance of CpNiNO^+ in reaction 2 as a function of wavelength at 10-nm resolution,¹² is compared in Figure 1 with the photoelectron spectrum of CpNiNO reported by Evans et al.⁹ The photodissociation spectrum represents an average of several runs, and the energy axis of the photoelectron spectrum is adjusted such that the first adiabatic ionization potential of CpNiNO is zero on the photodissociation energy scale.

As shown in Figure 1, there is an overlap between the photoexcitation curve and the state assigned by Evans et al. as arising from ionization from a C 2p σ type orbital having e_2 symmetry. This overlap suggests (but not unequivocally) that the observed transition at 4.13 eV (300 ± 10 nm) is ${}^2E_1 \rightarrow {}^2E_2$ (ligand-localized transition) electric dipole allowed along the x,y axes. In contrast, the photodissociation maximum in Figure 1 at 2.35 eV (530 ± 10 nm) does not overlap precisely with the photoelectron spectrum and suggests a transition of an electron to an unfilled orbital not detailed by PES. Alternatively, this behavior can be explained by the fact that the photodissociation band is in the vicinity of the thermodynamic threshold.⁶ The onset for photodissociation observed at 1.9 ± 0.1 eV (≈ 660 nm) yields an upper limit on the bond dissociation energy of $D(\text{NO-CpNi}^+) \leq 43 \pm 3$ kcal/mol, in good agreement with the photoionization results. The addition of collision gases was found to have no significant effect upon the threshold region.

In summary, photodissociation is a powerful method for yielding absorption information about gas-phase metal-ion complexes. This initial study also indicates the utility of

Received June 8, 1978